LM-04K066
August 4, 2004

Auger and Radiative Recombination Coefficients in 0.55 eV InGaAsSb

CA Wang, G Nichols

Auger and Radiative Recombination Coefficients in 0.55 eV InGaAsSb

R. J. Kumar, J. M. Borrego, P. S. Dutta, and R. J. Gutmann
Center for Integrated Electronics
Department of Electrical, Computer and Systems Engineering
Rensselaer Polytechnic Institute, Troy, NY 12180

C. A. Wang
Lincoln Laboratory
Massachusetts Institute of Technology
Lexington, MA 02420

G. Nichols
Lockheed Martin
Schenectady, NY 12301

Abstract

A radio-frequency (RF) photoreflectance technique, which senses changes in sample conductivity as carriers recombine following excitation by a laser pulse, has been used to measure the recombination parameters in 0.55 eV InGaAsSb lattice matched to GaSb. Doubly-capped lifetime structures with variable active layer thicknesses are used to extract the surface recombination velocity (SRV), while analysis of the samples with different doping concentrations is used to obtain Auger (C) and radiative (B) recombination parameters. Parameter extraction for the samples evaluated gives $C = 1 \pm 0.4 \times 10^{-28}$ cm^6/s and $B = 3 \pm 1.5 \times 10^{-11}$ cm^3/s for 0.55 eV InGaAsSb lattice matched to GaSb. The Auger and radiative recombination coefficients obtained from high-level injection decay times in low doping concentration samples show very good agreement with values obtained from low-level injection conditions.

1. Introduction

Antimonide-based semiconductors [1-2] have lattice constants close to 6.1 Angstroms and bandgaps corresponding to the infrared region of the electromagnetic spectrum. A wide range of electronic bandgaps, bandgap offsets and electronic barriers is possible with these materials. These properties and the high electron mobility in these materials enable a wide variety of optoelectronic and electronic devices [3-6]. Antimonide materials are also used in thermophotovoltaics, which involves the generation of electricity from a heat source using a semiconductor device [7-8]. For a radiator temperature of 800-1000 ^oC, the best compromise between power density and efficiency in a TPV device is obtained with a bandgap in the range of 0.50 to 0.60 eV [9]. High-quality TPV devices have been obtained with InGaAsSb epitaxial layers grown lattice matched to GaSb substrates [10-13].

Minority carrier lifetime is a critical parameter which determines the performance of these devices. Estimates of the recombination parameters for 0.55 eV InGaAsSb based on interpolation of reported data for III-V compounds gives a value between 10^{-29} cm^6/s and 10^{-26} cm^6/s for the Auger coefficient and between 10^{-11} cm^3/s and 10^{-10} cm^3/s for the radiative coefficient [9]. Bulk lifetime and surface recombination velocities (SRVs) in

InGaAsSb at specific doping concentrations have also been reported [14, 15]. In earlier work [16, 17] we reported initial results on the recombination coefficients in 0.50 to 0.59 eV InGaAsSb. In this paper we obtain more accurate estimates for the recombination parameters in 0.55 eV InGaAsSb using analysis of samples with a wider range of doping concentrations and different injection levels.

2. Measurement Technique and Lifetime Structures

A radio-frequency (RF) photoreflectance technique, which senses changes in sample conductivity as carriers recombine following excitation by a laser pulse, is used to measure the decay rate of carriers in the sample [14]. Earlier work has successfully applied this technique to characterize antimonide-based substrates and epitaxial layers using double-heterostructure confinement [14, 16-18]. A Q-switched Nd:YAG laser operating at 1064 nm with an energy of 1.5 mJ/pulse is used to excite carriers in the sample. The pulse width (full-width half-maximum) and decay time are 14 ns and 5 ns respectively. The total width of the pulse is approximately 40 ns. Carrier generation due to the laser pulse takes place from t = 20 ns to t = 60 ns in the photoresponse transients shown in the paper. The decay times of samples are measured after t = 60 ns to eliminate effect of optical generation on the measured decay times.

The InGaAsSb lifetime structures consist of a single 0.55 eV InGaAsSb p-type active layer with higher bandgap capping layers at the front and back, as shown in Figure 1. The layers are grown by organometallic vapor phase epitaxy, lattice matched to GaSb substrates [10]. The capping layers of GaSb (0.72 eV) or AlGaAsSb (~1 eV) limit the front and back SRVs to the order of ~ 10^3 cm/s [14].

For a thin doubly-capped structure with small SRVs (S_1, S_2 << D/W, where D is the diffusion coefficient of the minority cariers), the effective decay time of carriers in the active layer is the sum of contribution from bulk and surface recombination, as given by the equation [14],

$$\frac{1}{\tau_{eff}} = \frac{1}{\tau_B} + \frac{S_1 + S_2}{W} \qquad (1)$$

where τ_{eff} is the effective decay time of the carriers, τ_B is the bulk lifetime, S_1 and S_2 are the front and back SRVs and W is the thickness of the sample. Assuming low level injection conditions and $S_1 = S_2 = S$, bulk lifetime can be expressed as,

$$\frac{1}{\tau_{eff}} = \frac{1}{\tau_{Aug}} + \frac{1}{\tau_{Rad}} + \frac{1}{\tau_{SRH}} + \frac{2S}{W} = CN^2 + BN + \frac{1}{\tau_{SRH}} + \frac{2S}{W} \qquad (2)$$

In the above equation, τ_{Aug}, τ_{Rad}, τ_{SRH} are the Auger, Radiative and Shockley-Read-Hall (SRH) lifetimes, C is the Auger coefficient, B is the radiative recombination coefficient and N is the doping concentration.

Photon recycling [19-22] occurs when photons emitted during radiative recombination are reabsorbed within the semiconductor layer generating new electron-hole pairs. Photon recycling increases with increasing sample thickness and has the effect of prolonging the effective radiative component of the lifetime. The effect of photon recycling on radiative lifetime can be incorporated by including a 'photon recycling factor' ϕ, defined by the equation, $1/\tau_{Rad} = BN/\phi$, where ϕ depends on the thickness of the sample and is greater than 1. While the photon recycling factor is not explicitly

considered in this work, the radiative lifetimes obtained from the analysis would represent the longer lifetimes that result from any photon recycling in the samples, and the obtained effective radiative recombination coefficient (B_{eff}) would include the photon recycling factor (i.e., $B_{eff}=B/\phi$). The effect of photon recycling on the obtained recombination parameters is briefly discussed in Section 7.

Equations (1) and (2) show that epitaxial layers with different thicknesses (W) can be used to separate the effect of bulk lifetime and SRV. Samples with different doping concentrations (N) can be used to separate out the contribution from different mechanisms. Measurements were performed on four sets of 0.55 eV InGaAsSb samples with active layer doping concentrations of 1 x 10^{16} cm^{-3}, 2 x 10^{17} cm^{-3}, and 1 x 10^{18} cm^{-3}, and different capping layers, as shown in Table 1.

3. Simulation of Photoconductivity Response

Analysis and/or simulation techniques are required to isolate bulk and surface effects with the lifetime structures. A one-dimensional device simulation tool (PC-1D®) is used to model the sheet conductance transient response to above-bandgap optical excitation [23]. The material and recombination parameters of the sample are specified, and the integrated conductivity transient in response to the laser pulse is assumed proportional to the RF photoresponse signal obtained from the sample. PC-1D® is also used to plot the electron and hole concentrations in the sample in response to the laser pulse and to determine the injection levels.

Use of one-dimensional simulations to evaluate the photoconductivity response of the lifetime structures to the optical injection pulse has been reported in detail earlier [16]. Simulations show that the peak hole concentration in the epitaxial samples is approximately 10^{18} cm^{-3} for laser pulse energy of 1.5 mJ. For the 2 x 10^{17} cm^{-3} doped samples shown in Table 1, the hole concentration decreases to < 2.3 x 10^{17} cm^{-3} for t = 150 ns or greater (after the laser excitation). The 2 x 10^{17} cm^{-3} and 1 x 10^{18} cm^{-3} doped samples are in low-level injection (LLI) conditions when the decay times are measured, and the electron concentrations in the samples are less than 1/10 of the hole concentrations. For the 5-μm thick 1 x 10^{16} cm^{-3} doped sample (01-448), the electron and hole concentrations are comparable and greater than the doping concentration for more than 500 ns following the optical excitation; therefore this sample is under high-level injection (HLI) conditions when the decay times are measured.

4. Experimental Results

RF photoreflectance measurements were performed on the four sets of samples shown in Table 1. The photoresponse obtained from the 01-484 to 01-488 series samples (2 x 10^{17} cm^{-3} doped active layers and AlGaAsSb capping layers) at 1064 nm and pulse energy of 1.5 mJ is shown in Figure 2. The amplitude of the photoresponse as well as the decay time increases with increasing sample thickness. The decay time increases due to the smaller amount of surface recombination with increasing thickness as shown by equation (2). The inverse of the decay times is plotted against the inverse active layer thicknesses and the best straight line fit through the points is obtained (Figure 3). The bulk lifetime and surface recombination velocity for the sample series can be obtained as: SRV = slope / 2, bulk lifetime = 1 / y-intercept. The 01-484 to 01-488 series shows bulk lifetime = 81 ns and SRV = 680 cm/s.

The 01-506 to 01-510 series consists of samples with 2 x 10^{17} cm^{-3} doped p-InGaAsSb active layers and 2 x 10^{18} cm^{-3} doped p-GaSb capping layers. The decay times of the samples vary from 27 ns to 54 ns (Table 2), and are approximately 20 ns shorter than the decay times of samples with AlGaAsSb capping layers. Plotting the inverse decay times against the inverse active layer thicknesses gives bulk lifetime = 100 ns and SRV = 1350 cm/s. The bulk lifetime of is comparable to that of the 01-484 to 01-488 series (81 ns), but the SRV is almost twice the value obtained (680 cm/s) for the AlGaAsSb capped samples. The extraction of B and C coefficients compatible with the decay times of the above samples is discussed in Section 5.

The photoresponse obtained with the 10^{18} cm^{-3} doped sample (98-817) is shown in Figure 4. The sample has a decay time of approximately 8 ns. The low decay time measured for the 10^{18} cm^{-3} doped sample could be attributed to the low Auger lifetime at this high doping concentration. The analysis of the 2 x 10^{17} cm^{-3} and 1 x 10^{18} cm^{-3} doped samples to obtain the B and C coefficients is discussed in Section 5.

01-448 is a 5 μm thick unintentionally doped (10^{16} cm^{-3}) p-InGaAsSb sample with unintentionally doped (10^{16} cm^{-3}) GaSb capping layers. The photoresponse of the sample at 1064 nm and 1.5 mJ pulse energy is also shown in Figure 4. As mentioned in Section 3, a sample doped at 10^{16} cm^{-3} is in high-level injection condition for more than 500 ns after the laser excitation. The decay times of the sample at t = 100 ns, 150 ns, 200 ns and 300 ns are 62 ns, 110 ns, 160 ns and 215 ns respectively. The simulation of the photoresponse of this sample is discussed in Section 6.

5. Extraction of Recombination Coefficients using Doped Samples

This section describes the extraction of B and C coefficients from the decay times of the 2 x 10^{17} cm^{-3} and 10^{18} cm^{-3} doped samples. The SRV is obtained from active layers with different thicknesses as explained in Section 4, and a value of 1 μs is assumed for the SRH lifetime in accordance with recent results on undoped p-type epitaxial samples [11]. The known values of SRV and SRH lifetime can be used to determine the B and C coefficients compatible with the decay time of a sample. The 3 μm thick sample 01-486 (with 2 x 10^{17} cm^{-3} p-doped active layer and AlGaAsSb capping layer) with decay time of 53 ns is used to describe the methodology.

Figure 5 shows the PC-1D® simulation transients for three different sets of radiative (B) and Auger (C) coefficients: B = 1 x 10^{-11} cm^3/s, C = 5 x 10^{-29} cm^6/s; B = 3 x 10^{-11} cm^3/s, C = 10^{-28} cm^6/s; and B = 5 x 10^{-11} cm^3/s, C = 3 x 10^{-28} cm^6/s used initially to simulate sample 01-486. An SRV of 680 cm/s is used based on the results in Section 4 and a value of 1 μs is used for the SRH lifetime [11]. The three sets of B and C coefficients give decay times of 78 ns, 53 ns and 32 ns respectively. Figure 5 shows the sensitivity of the decay times to the values of B and C coefficients, and that the combination B = 3 x 10^{-11} cm^3/s and C = 1 x 10^{-28} cm^6/s satisfies the decay time of 53 ns observed for the 3 μm sample.

Since more than one combination of B and C coefficients can result in a decay time of 53 ns, the combination of B and C values which result in a given decay time can be determined as follows. The effective decay time due to the different recombination mechanisms can be written as,

$$\frac{1}{\tau_{eff}} = \frac{1}{\tau_{Rad-Aug}} + \frac{1}{\tau_{SRH}} + \frac{2S}{W} = CP^2 + BP + \frac{1}{\tau_{SRH}} + \frac{2S}{W} \qquad (3)$$

where

$$\frac{1}{\tau_{Rad-Aug}} \equiv \frac{1}{\tau_{Rad}} + \frac{1}{\tau_{Aug}}$$

Since τ_{eff}, τ_{SRH}, S and W are known, $\tau_{Rad\text{-}Aug}$ can be written as,

$$\frac{1}{\tau_{Rad-Aug}} = BP + CP^2 = \frac{1}{\tau_{eff}} - \frac{1}{\tau_{SRH}} - \frac{2S}{W} \qquad (4)$$

With τ_{eff} = 53 ns, τ_{SRH} = 1 μs, S = 680 cm/s and W = 3 μm, equation (4) gives $\tau_{Rad\text{-}Aug}$ = 75 ns. Simulations show that the hole concentration in the sample at t=150 ns following the laser excitation is approximately 2.3 x 10^{17} cm^{-3}. The possible B and C coefficients which give $\tau_{Rad\text{-}Aug}$ = 75 ns can be obtained by plotting the Auger coefficient versus the radiative coefficient using the expression $BP + CP^2$ = 1/75 ns, with P = 2.3 x 10^{17} cm^{-3}. This procedure can be applied to the other four samples with AlGaAsSb capping layers (1.2 μm, 1.5 μm, 2.1 μm and 5 μm thick), as well as the 01-506 to 01-510 series (2 x 10^{17} cm^{-3} doped active layers and p-GaSb capping layers). Very good agreement is obtained between the results for AlGaAsSb capped samples and also between p-GaSb and AlGaAsSb capped samples. The solid lines in Figure 6 show the plots of radiative and Auger coefficients obtained for five 2 x 10^{17} cm^{-3} doped samples (01-486, 01-487, 01-488 with AlGaAsSb caps and 01-508, 01-509 with p-GaSb caps).

Decay times of samples with different doping concentrations are required to determine the B and C coefficients. If only two samples with two different doping concentrations are considered, the point at which the B vs. C curves for the two samples intersect would give the B, C values satisfying the decay times of both samples. But since there are multiple samples with 2 x 10^{17} cm^{-3} doping concentration and these samples show a spread in the extracted B vs. C curves, we need to consider a range of values for the B and C coefficients.

The 10^{18} cm^{-3} doped sample (98-817) has a decay time of 8 ns as shown in Figure 4. Simulations show that the hole concentration in the sample decreases to the background doping concentration of 10^{18} cm^{-3} for t > 60 ns, and the sample is in LLI condition. The combinations of B and C coefficients satisfying the 8 ns decay time calculated using equation (4), assuming P = 10^{18} cm^{-3} and SRV = 10^3 cm/s, is indicated by the dashed line in Figure 6. The curve for the 10^{18} cm^{-3} doped sample intersects the set of curves for the 2 x 10^{17} cm^{-3} doped samples for B = 2 to 4 x 10^{-11} cm^3/s, C = 0.7 to 1.2 x 10^{-28} cm^6/s. Therefore, the range of B and C coefficients consistent with the measured decay times of the samples is B ≈ 3 ± 1 x 10^{-11} cm^3/s, and C ≈ 1.0 ± 0.3 x 10^{-28} cm^6/s. This range of values is indicated in Figure 6.

6. Simulation of unintentionally doped (10^{16} cm^{-3}) sample using the obtained recombination parameters

In this section, the photoresponse of the unintentionally (10^{16} cm^{-3}) doped sample 01-448 is simulated using the B and C coefficients obtained in Section 5. The decay times observed with the sample at t = 100 ns, 150 ns, 200 ns and 300 ns are 62 ns, 110 ns, 160

ns and 215 ns, respectively as shown in Figure 4. Unlike the 2 x 10^{17} cm^{-3} and 10^{18} cm^{-3} doped samples, the unintentionally doped sample is in high-level injection conditions (comparable electron and hole concentrations) when the decay times are measured, due to the low doping concentration. Noise limitations of the current experimental set-up prevent measurements of the undoped samples at lower injection levels.

Modifications in SRH lifetime, Auger lifetime, and SRV under HLI conditions are considered as follows. The SRH lifetime under HLI conditions is the sum of the LLI electron and hole SRH lifetimes. Measurements on undoped (10^{16} cm^{-3}) p-InGaAsSb epitaxial samples show an electron SRH lifetime of approximately 1 μs in p-type materials [11]; a value of 1 μs is also assumed for the hole lifetime. Similarly, the effective SRV decreases and the surface lifetime increases under HLI conditions. Dhariwal et al. [24] have obtained an effective SRV, $(S_{eff})_{HLI} = (1/2)(S_n S_p)^{1/2}$; assuming $S_n = S_p$, $(S_{eff})_{HLI} = (1/2)S_p$. For the simulations, the low-level SRH lifetimes and SRVs are specified, and the models in PC-1D® incorporate the above modifications for HLI conditions.

Under HLI conditions, the effective Auger coefficient is the sum of the Auger coefficients under LLI conditions (C_n and C_p). Calculations by Flatte and Grein [25-27] show no significant difference between values of C_n and C_p for antimonide-based materials. The simulations done here assume $C_n = C_p = C$ and a value of 2C is used as the Auger coefficient under HLI conditions. The above modifications for the parameters are included in the models for simulating the HLI photoresponse of the sample.

The photoresponse of the unintentionally doped sample is simulated using PC-1D® with the B and C coefficients (B = 3 x 10^{-11} cm^3/s, C = 10^{-28} cm^6/s) obtained in Section 5 using the 2 x 10^{17} cm^{-3} and 10^{18} cm^{-3} doped samples. A low-level injection SRV of 1000 cm/s is used based on the average of SRVs obtained for 2 x 10^{17} cm^{-3} InGaAsSb active layers with AlGaAsSb (680 cm/s) and p-GaSb (1350 cm/s) capping layers, and a SRH lifetime (LLI) of 1 μs is specified. The simulated photoconductivity response as well as the experimental photoresponse of the sample are shown in Figure 7. The figure shows very good agreement between the two curves between t = 100 ns and t = 500 ns. Therefore, the B and C coefficients obtained by considering the decay times of the doped samples under LLI conditions are compatible with the photoresponse obtained for the unintentionally doped sample under HLI conditions.

7. Consideration of Photon Recycling

The above analysis does not take into account the photon recycling factor for calculation of the recombination coefficients. The effect of photon recycling increases with increasing sample thickness, with the longer decay times in thicker samples attributed to a longer effective radiative lifetime due to a larger photon recycling factor. The above analysis assumes that the slope of the $1/\tau_{eff}$ vs. 1/W plot for samples with different thicknesses is entirely due to surface recombination (for example, Figure 3). In the presence of photon recycling, the actual SRV at the interface is lower than the value obtained from the slope of the straight line fit [21]. Since the effective B coefficient obtained from our data analysis includes the photon recycling factor, the real radiative recombination coefficient in the material would be larger than the value estimated above (i.e., $B=\phi B_{eff}$). The decrease in inverse decay time with the thicker (5 μm) sample shown in Figure 3 is compatible with photon recycling being significant in this sample. Recent

results with other samples showing appreciable photon recycling indicate comparable values for B and C as obtained here [28].

8. Uncertainty in Parameter Extraction

The uncertainty in evaluation of the recombination parameters due to errors and uncertainties in the measurement setup and sample parameters is briefly discussed below. Assuming statistical independence, the final error in the values of B and C is the square root of the sum of the square of errors due to each of the different factors. Extensive measurements of lifetime samples using the RF photoreflectance system show that the repeatability in measuring the photoresponse and estimating the decay time of a sample is within 5%, while the error in estimating the surface recombination velocity from $1/\tau_{eff}$ vs. 1/W plots is approximately 10% for the sample thicknesses used in this research. The measured doping concentrations in the epitaxial samples are accurate to within ±10 %. Analysis shows that an error of 10% in the doping concentration results in an error of approximately 20% in the estimates for B and C. Analysis also shows that a factor of 2 error in SRH lifetime (from the assumed value of 1 μs) would result in a change in B and C coefficients of approximately 10 %.

There is an uncertainty in the estimation of B and C due to the range of values obtained from different sample series. Assuming the baseline parameters, $C = 1 \times 10^{-28}$ cm^6/s and $B = 3 \times 10^{-11}$ cm^3/s, the range of Auger and radiative coefficients from the different samples are approximately 30% and 40% respectively, as obtained in Section 5. Combining the error above with the 5 % error due to repeatability and decay time estimation in the RF photoreflectance system, the 10% error due to SRV estimation, the 10% error due to possible error in SRH lifetime and 20% error in B and C due to doping concentration uncertainty, results in a net uncertainty of ≈ 40% for the Auger coefficients and of ≈ 50% for the Radiative recombination coefficients. Therefore, $C = (1 \pm 0.4) \times 10^{-28}$ cm^6/s and $B = (3 \pm 1.5) \times 10^{-11}$ cm^3/s for 0.55 eV InGaAsSb lattice-matched to GaSb ($In_{0.15}Ga_{0.85}As_{0.14}Sb_{0.86}$). Including the effects of photon recycling would require small changes in the obtained SRV and radiative coefficient. However since most of our results are with epitaxial layers ≤ 4 μm where photon recycling is not a major factor, we believe that B (not only B_{eff}) is within the quoted range for 0.55 eV InGaAsSb lattice-matched to GaSb.

9. Device Implications and Summary

The Auger, radiative, SRH and net low-level injection bulk lifetime (with $C = 1 \times 10^{-28}$ cm^6/s, $B = 3 \times 10^{-11}$ cm^3/s and SRH lifetime = 1 μs) for doping concentration (P) ranging from 10^{15} cm^{-3} to 10^{19} cm^{-3} is shown in Figure 8. The figure shows that for $P = 2 \times 10^{17}$ cm^{-3}, the low-level injection bulk lifetime is ≈ 90 ns, which is in very good agreement with the value of 95 ns obtained by Saroop et al. [14] for 2×10^{17} cm^{-3} doped InGaAsSb samples. The obtained B and C coefficients show good agreement with recently reported lifetime results on InGaAsSb [28, 29]. The key lifetime limiting mechanisms as a function of doping concentration are summarized in Table 3.

While quantitative evaluation of recombination parameters has been emphasized herein, the research is motivated by the impact on the design and performance of minority carrier devices. Peak internal quantum efficiency greater than 90% has been reported on epitaxially grown 0.55 eV InGaAsSb TPV cells with AlGaAsSb window

layers [30]. The quantum efficiency of a 0.55 eV InGaAsSb TPV cell was simulated using the obtained radiative and Auger coefficients. The simulated cell had a 5 μm thick 2 x 10^{17} cm^{-3} p-InGaAsSb emitter, a 1 μm thick 5 x 10^{17} cm^{-3} n-InGaAsSb base and a 500 μm thick 2 x 10^{17} cm^{-3} n-GaSb substrate. The peak internal QE of ≈ 90% observed in the simulations with the obtained recombination parameters is in agreement with the experimental QE results [31]. While higher doping concentration in the p-type emitter is desirable for lower contact resistance, the lower lifetime depicted in Figure 8 leads to reduced TPV cell performance.

In summary, RF photoreflectance measurements, one-dimensional simulations and analysis on p-type InGaAsSb lifetime structures with GaSb and AlGaAsSb capping layers give an Auger coefficient, C, = (1 ± 0.4) x 10^{-28} cm^6/s and a radiative recombination coefficient, B, = (3 ± 1.5) x 10^{-11} cm^3/s for 0.55 eV p-type InGaAsSb lattice matched to GaSb. The B and C coefficients obtained from analysis of decay times at high-level injection conditions in the unintentionally doped sample show good agreement with the values obtained from low-level injection decay times using samples with different doping concentrations. The obtained recombination parameters are compatible with reported quantum efficiency results in InGaAsSb TPV cells, and provide useful information for TPV device design.

Acknowledgments

The authors would like to thank Dr. Sudesh Saroop (formerly at RPI and now at IBM) for development of the RF photoreflectance setup and previous characterization.

References

[1]. P. S. Dutta, H. L. Bhat, and V. Kumar, Journal of Applied Physics, Volume 81, Number 9, pp. 5821 - 5870 (May 1997).

[2]. M. O. Manasreh (editor), “Antimonide-Related Strained-layer Heterostructures”, Gordon and Beach Science Publishers (1997).

[3]. D. C. Kilper, F. Quochi, J. E. Cunningham, M. Dinu, IEEE Photonics Technology Letters, Volume 14, Issue 4, pp. 438 - 440 (April 2002).

[4]. X. Marcadet, A. Rakovska, I. Prevot, G. Glastre, B. Vinter, V. Berger, Journal of Crystal Growth, Volumes 227-228, pp. 609 - 613 (July 2001).

[5]. C. Lin, Y. L. Zheng, A. Z. Li, Journal of Crystal Growth, Volume 227-228, pp. 605 - 608 (July 2001).

[6]. C. R. Bolognesi, M. M. W. Dvorak, P. Yeo, X. G. Xu, S. P. Watkins, IEEE Transactions on Electron Devices, Volume 48, Issue 11, pp. 2631 - 2639 (Nov 2001).

[7]. T. Coutts and M. Fitzgerald, "Thermophotovoltaics", Scientific American, pp. 90 - 95 (September 1998).

[8]. K. Barnham, J. Connolly, and C. Rohr (editors), Special Issue on Thermophotovoltaics, Semiconductor Science and Technology, Volume 18, Number 5 (May 2003).

[9]. G. W. Charache, P. F. Baldasaro, L. R. Danielson, D. M. DePoy, M. J. Freeman, C. A. Wang, H. K. Choi, D. Z. Garbuzov, R. U. Martinelli, V. Khalfin, S. Saroop, J. M. Borrego, and R. J. Gutmann, Journal of Applied Physics, Volume 85, Number 4, pp. 2247 - 2252 (February 1999).

[10]. C. A. Wang, H. K. Choi, and G. W. Charache, IEE Proceedings: Optoelectronics, Vol. 147, No. 3, pp. 193 - 198 (June 2000).
[11]. C. A. Wang, C. J. Vineis, H. K. Choi, M. K. Connors, R. K. Huang, L. R. Danielson, G. Nichols, G. W. Charache, D. Donetsky, S. Anikeev and G. Belensky, Proceedings of Thermophotovoltaic Generation of Electricity: 5th Conference, American Institute of Physics, pp. 324 - 334 (2003).
[12]. C. W. Hitchcock, R. J. Gutmann, H. Ehsani, I.B. Bhat, C.A. Wang, M.J. Freeman, and G.W. Charache, Journal of Crystal Growth, Volume 195, Number 1-4, pp. 363 - 372 (December 1998).
[13]. C. W. Hitchcock, R. J. Gutmann, J. M. Borrego, I. B. Bhat, and G. W. Charache, IEEE Transactions on Electron Devices, Volume 46, Number 10, pp. 2154 - 2161 (October 1999).
[14]. S. Saroop, J. M. Borrego, R. J. Gutmann, G. W. Charache, and C. A. Wang, Journal of Applied Physics, Volume 86, Number 3, pp. 1527 - 1534 (August 1999).
[15]. D. Donetsky, S. Anikeev, G. Belenky, S. Luryi, C. A. Wang and G. Nichols, Applied Physics Letters, Volume 81, Issue 25, pp. 4769 - 4771 (December 2002).
[16]. R. J. Kumar, R. J. Gutmann, J. M. Borrego, P. S. Dutta, C. A. Wang, R. U. Martinelli and G. Nichols, Journal of Electronic Materials, Volume 33, Number 2, pp. 94-100 (February 2004).
[17]. R. J. Kumar, R. J. Gutmann, J. M. Borrego, P. S. Dutta, C. A. Wang, R. U. Martinelli and G. Nichols, MRS Spring 2003 Proceedings, Volume 763, B2.4 (2003).
[18]. R. K. Ahrenkiel, Proceedings of the 1997 IEEE 26th Photovoltaic Specialists Conference, Anaheim, CA, pp. 119 - 122 (1997).
[19]. P. Asbeck, Journal of Applied Physics, Volume 48, Number 2, pp. 820-822 (February 1977)
[20]. G. B. Lush, M. R. Melloch, M. S. Lundstrom, D. H. Levi, R. K. Ahrenkiel, and H. F. MacMillan, Applied Physics Letters, Volume 61, Number 20, pp. 2440 – 2442 (November 1992).
[21]. J. M. Borrego, S. Saroop, R. J. Gutmann, G. W. Charache, T. Donovan, P. F. Baldasaro, and C. A. Wang, Journal of Applied Physics, Volume 89, Number 7, pp. 3753 – 3759 (April 2001).
[22]. S. Anikeev, D. Donetsky, G. Belenky, S. Luryi, C. A. Wang, J. M. Borrego, and G. Nichols, Applied Physics Letters, Volume 83, Number 16, pp. 3317-3319 (October 2003)
[23]. D. A. Clugston and P. A. Basore, Proceedings of the 26th IEEE Photovoltaic Specialists Conference, IEEE, New York, pp. 207 – 210 (1997).
[24]. S. R. Dhariwal and D. R. Mehrotra, Solid State Electronics, Volume 31, Number 9, pp. 1355 - 1361 (September 1988).
[25]. Private conversation between Prof. M. E. Flatté and Prof. R. J. Gutmann (2002).
[26]. M. E. Flatté, C. H. Grein, H. Ehrenreich, R. H. Miles, and H. Cruz, Journal of Applied Physics, Volume 78, Number 7, pp. 4552 - 4559 (October 1995).
[27]. C. H. Grein, P. M. Young, M. E. Flatté and H. Ehrenreich, Journal of Applied Physics, Volume 78, Number 12, pp. 7143 - 7152 (December 1995).
[28]. J. M. Borrego, R. J. Gutmann, R. J. Kumar, C. A. Wang, G. Nichols, H. Ehsani, and J. F. Beausang, Journal of Applied Physics, under submission, (May 2004).
[29]. I. Riech, P. Diaz, and E. Marin, Phys. Stat. Sol. (b), Volume 220, pp. 305 - 309 (July 2000).

[30]. H. K. Choi, C. A. Wang, G. W. Turner, M. J. Manfra, D. L. Spears, G. W. Charache, L. R. Danielson, and D. M. Depoy, Applied Physics Letters, Volume 71, Number 26, pp. 3758 - 3760 (December 1997).
[31]. J. M. Borrego, C. A. Wang, P. S. Dutta, G. Rajagopalan, R. J. Gutmann, I. B. Bhat, H. Ehsani, J. F. Beausang, G. Nichols, and P. F. Baldasaro, Proceedings of Thermophotovoltaic Generation of Electricity: 5th Conference, American Institute of Physics, pp. 498 – 507 (2003).

Tables

Sample / Sample Series	Active Layer Thickness	Active Layer Doping	Capping Layer
01-448	5 μm	1 x 10^{16} cm^{-3}	1 x 10^{16} cm^{-3} p-GaSb
01-484 to 01-488	1.2 μm to 5 μm	2 x 10^{17} cm^{-3}	2 x 10^{17} cm^{-3} p-AlGaAsSb
01-506 to 01-510	1.2 μm to 4 μm	2 x 10^{17} cm^{-3}	2 x 10^{18} cm^{-3} p-GaSb
98-817	3 μm	1 x 10^{18} cm^{-3}	1 x 10^{16} cm^{-3} p-GaSb

Table 1. Structure of 0.55 eV InGaAsSb samples with variable doping concentration

Sample	Thickness (μm)	Decay Time (ns)
01-506	1.2	27
01-507	1.5	36
01-508	2	46
01-509	3	51
01-510	4	54

Table 2. Sample active layer thicknesses and observed decay times for 01-506 to 01-510 series

Doping Concentration (P)	LLI-limiting mechanism(s)	LLI Lifetime
< 10^{16} cm^{-3}	Shockley-Read-Hall (SRH)	1 μs
3 x 10^{16} cm^{-3}	SRH and Radiative	500 ns
10^{17} cm^{-3}	Radiative	200 ns
3 x 10^{17} cm^{-3}	Radiative and Auger	50 ns
> 10^{18} cm^{-3}	Auger	< 8 ns

Table 3. LLI-limiting mechanism(s) for InGaAsSb lattice-matched to GaSb

Figures

p-type GaSb or AlGaAsSb capping layer	~ 100 nm
p-type 0.55 eV InGaAsSb active layer	1 to 5 μm
p-type GaSb or AlGaAsSb capping layer	~ 100 nm
n-GaSb substrate	~ 500 μm

Figure 1. Schematic of an InGaAsSb lifetime structure grown lattice-matched to GaSb substrate

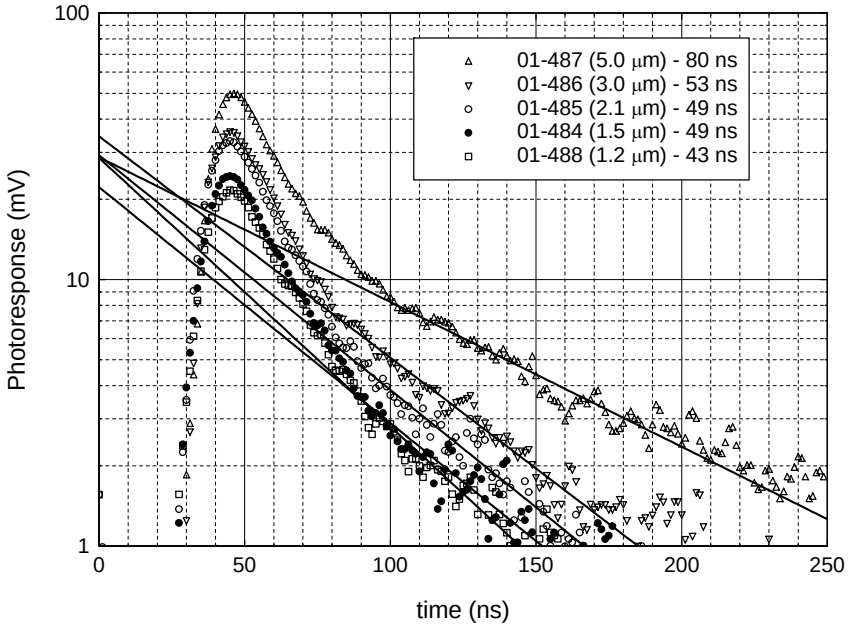

Figure 2. Photoresponse of samples with 2 x 10^{17} cm^{-3} doped active layers and AlGaAsSb capping layers (01-484 to 01-488 series)

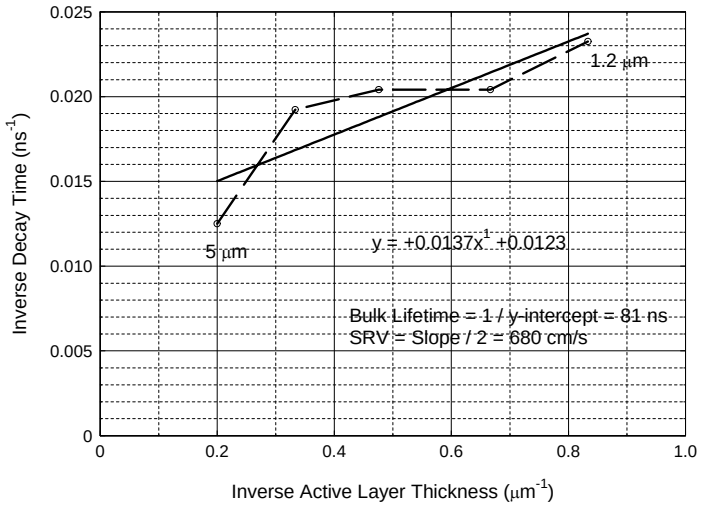

Figure 3. Extraction of bulk lifetime and SRV for series 01-484 to 01-488

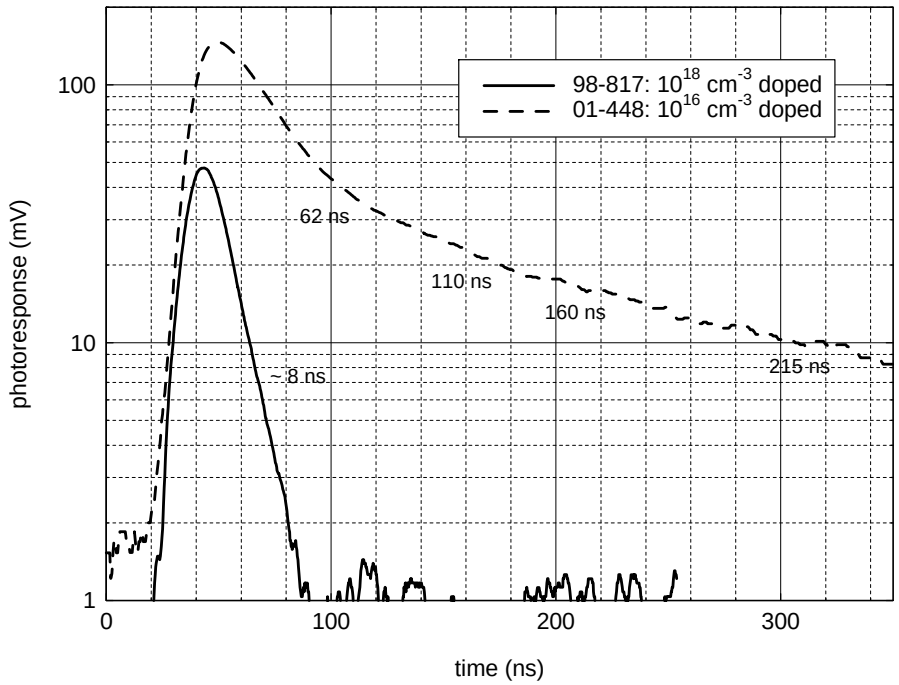

Figure 4. Photoresponse and decay times of the 3 μm thick 10^{18} cm^{-3} doped sample (98-817) and 5 μm thick 10^{16} cm^{-3} doped sample (01-448)

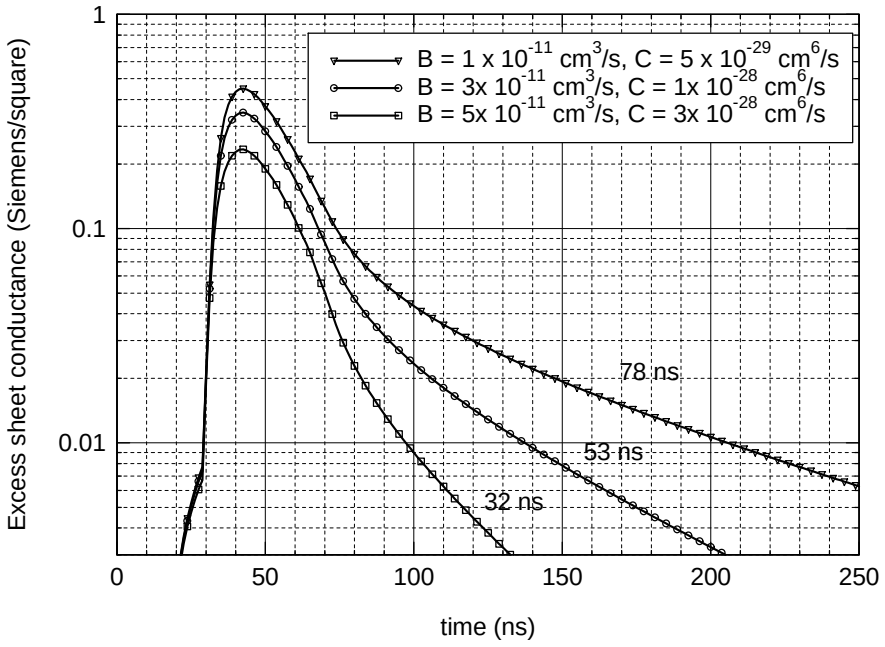

Figure 5. Simulated transients for the 3 μm thick sample for three different sets of radiative (B) and Auger (C) coefficients (SRV = 680 cm/s, τ_{SRH} = 1 μs)

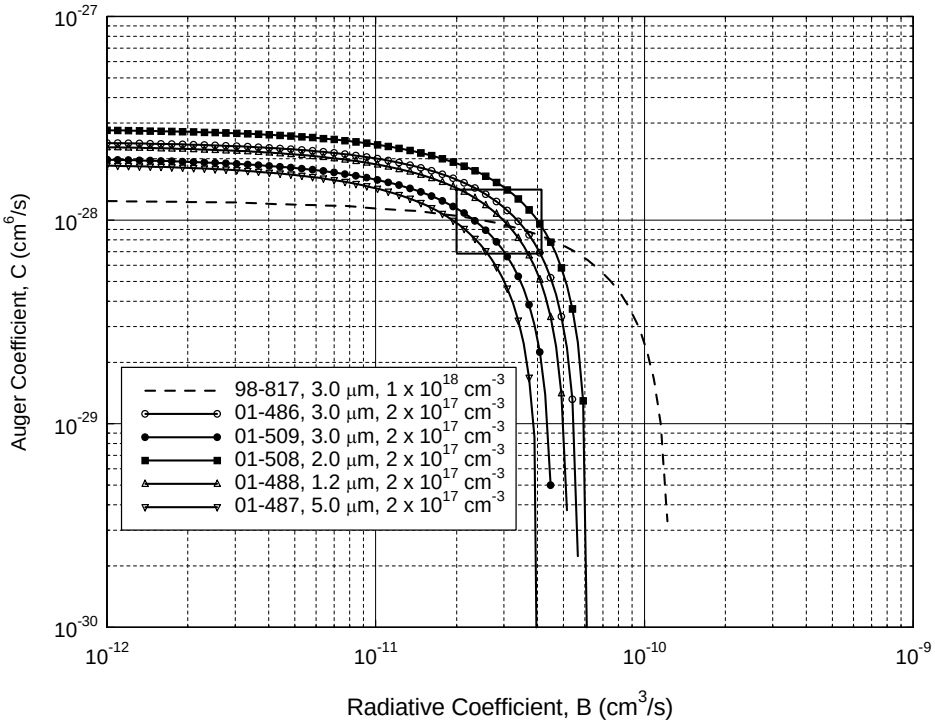

Figure 6. Combinations of B and C coefficients satisfying the observed decay times for 2 x 10^{17} cm^{-3} and 10^{18} cm^{-3} doped samples

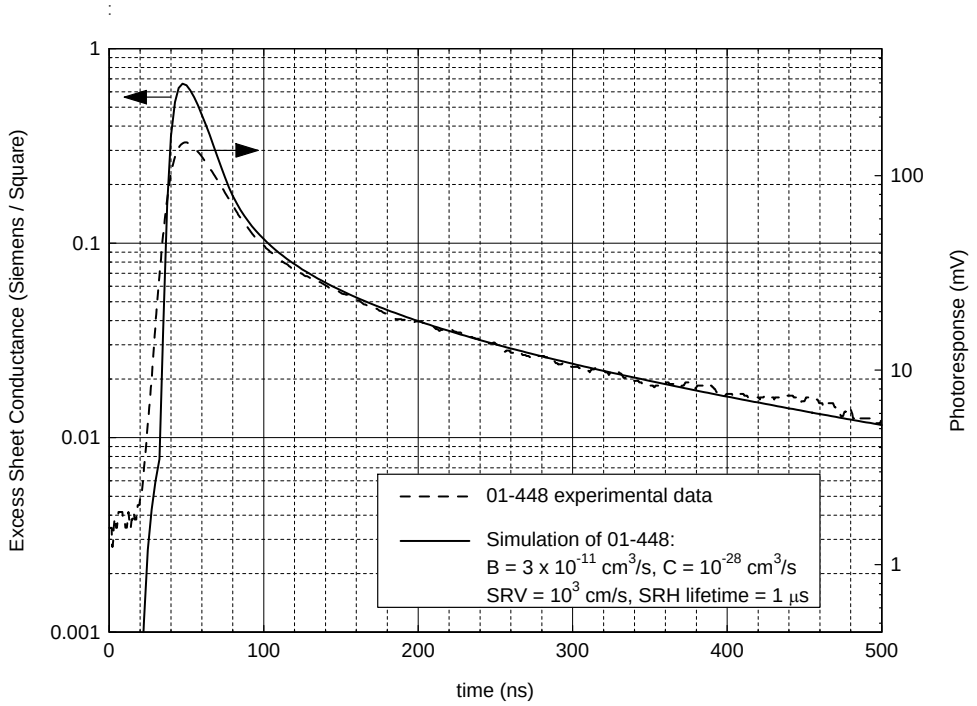

Figure 7. Experimental photoresponse and simulated photoconductivity response of 5 μm thick unintentionally doped sample (01-448).

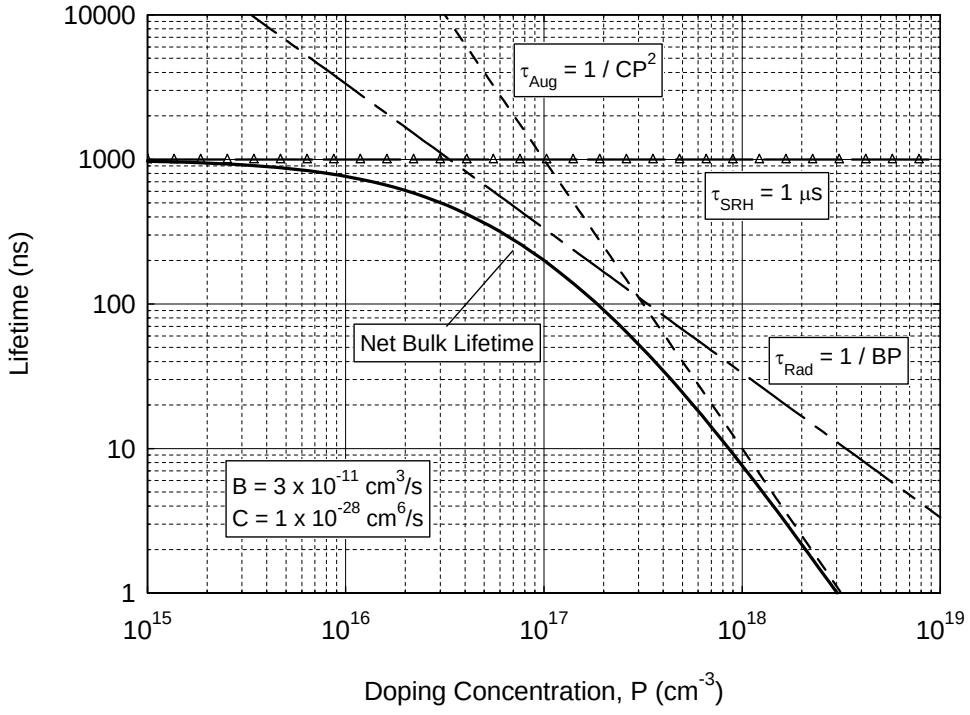

Figure 8. Auger, radiative, SRH and net low-level injection bulk lifetime vs. doping concentration for the obtained recombination parameters